Behind-the-Meter Storage

Anthony Burrell
National Renewable Energy Laboratory
15013 Denver West Parkway
Golden, CO 80401
Phone: (303) 384-6666
E-mail: anthony.burrell@nrel.gov

Samuel Gillard, DOE-EERE-VTO
Technology Manager, Battery R&D
Phone: (202) 287-5849
E-mail: samuel.gillard@ee.doe.gov

Start Date: 1 October 2018   End Date: 30 September 2022

Table of Contents

Project Introduction

This initiative, referred to as Behind-the-Meter Storage (BTMS), will focus on novel critical-materials-free battery technologies to facilitate the integration of electric vehicle (EV) charging, solar power generation technologies, and energy-efficient buildings while minimizing both costs and grid impacts. For extreme fast-charging at levels of 350 kW or higher, novel approaches are required to avoid significant negative cost and resiliency impacts. However, it is reasonable to assume that BTMS solutions would be applicable to other intermittent renewable energy generation sources or short-duration, high power-demand electric loads. BTMS research is targeted at developing innovative energy-storage technology specifically optimized for stationary applications below 10 MWh that will minimize the need for significant grid upgrades. Additionally, avoiding excessive high-power draws will eliminate excess demand charges that would be incurred during 350-kW fast-charging using current technologies. The key to achieving this is to leverage battery storage solutions that can discharge at high power but be recharged at standard lower power rates, acting as a power reservoir to bridge to the grid and other on-site energy generation technologies such as solar photovoltaics (PV), thereby minimizing costs and grid impacts. To be successful, new and innovative integration treatments must be developed for seamless interaction between stationary storage, PV generation, building systems, and the electric grid.

Key components of BTMS will address early-stage research into new energy-generation and building-integration concepts, critical-materials-free battery energy-storage chemistries, and energy-storage designs

with a focus on new stationary energy-storage strategies that will balance performance and costs for expanded fast-charging networks while minimizing the need for grid improvements.

Objectives

A cohesive multidisciplinary research effort to create a cost-effective, critical-materials-free solution to BTMS by employing a whole-systems approach will be taken. The focus of this initiative is to develop innovative battery energy-storage technologies with abundant materials applicable to EVs and high-power charging systems. Solutions in the 1–10 MWh range will eliminate potential grid impacts of high-power EV charging systems as well as lower installation costs and costs to the consumer.

Although many lessons learned from EV battery development may be applied to the BTMS program, the requirements for BTMS systems are unique—carrying their own calendar-life, cycle-life, and cost challenges. For example, EV energy-storage systems need to meet very rigorous energy-density and volume requirements to meet consumer transportation needs. Despite that, current stationary storage systems use batteries designed for EVs due to high volumes driving down costs. This creates another market demand for EV batteries, further straining the EV battery supply chain and critical-material demand.

By considering BTMS electrochemical solutions optimized for these applications with less focus on energy density in mass and volume, the potential for novel battery solutions is very appealing. Furthermore, the balance-of-plant (BOP) for a BTMS battery system, or the cost of everything minus the battery cells, is thought to be upwards of 60% of the total energy-storage system cost. In contrast, the EV's BOP costs make up roughly 30% of the total battery cost. Therefore, BTMS will also need to focus on reducing BOP cost through system optimization to realize desired cost targets.

The design parameters are needed to optimize the BTMS system for performance, reliability, resilience, safety, and cost.

The objectives for the project are to:

- Produce BTM battery solutions that can be deployed at scale and meet the functional requirement of high-power EV charging.

- Use a total-systems approach for battery storage to develop and identify the specific functional requirements for BTMS battery solutions that will provide novel battery systems in the 1–10 MWh range at $100/kWh installed cost—and able to cycle twice per day, discharging for at least 4 hours, with a lifetime of roughly 20 years or at least 8,000 cycles.

Approach

A cohesive multidisciplinary research effort—involving NREL, INL, SNL, and ORNL—will create a cost-effective, critical-materials-free solution to BTMS by employing a whole-systems approach. The focus of this initiative is to develop innovative battery energy-storage technologies with abundant materials applicable to PV energy generation, building energy-storage systems, EVs, and high-power charging systems. Solutions in the 1–10 MWh range will enable optimal integration of PV generation from a DC-DC connection, increase energy efficiency of buildings, eliminate potential grid impacts of high-power EV charging systems, and lower installation costs and costs to the consumer.

Many lessons learned from EV battery development may be applied to the BTMS program, but the requirements for BTMS systems are unique—carrying their own calendar-life, cycle-life, and cost challenges. For example, EV energy-storage systems need to meet very rigorous energy-density and volume requirements to meet consumer transportation needs. Despite that, current stationary storage systems use batteries designed for EVs due to high volumes that drive down the costs. This creates another market demand for EV batteries, further straining the EV battery supply chain and critical-material demand.

By considering BTMS electrochemical solutions optimized for these applications with less focus on energy density in mass and volume, the potential for novel battery solutions is very appealing. Furthermore, the BOP

for a BTMS battery system, or the cost of everything minus the battery cells, is thought to be upwards of 60% of the total energy-storage system cost. In contrast, the EV's BOP costs make up roughly 30% of the total battery cost. Therefore, BTMS will also need to focus on reducing BOP cost through system optimization to realize desired cost targets.

Integration of battery storage with PV generation, energy-efficient buildings, charging stations, and the electric grid will enable new and innovative control strategies. The design parameters are needed to optimize the BTMS system for performance, reliability, resilience, safety, and cost.
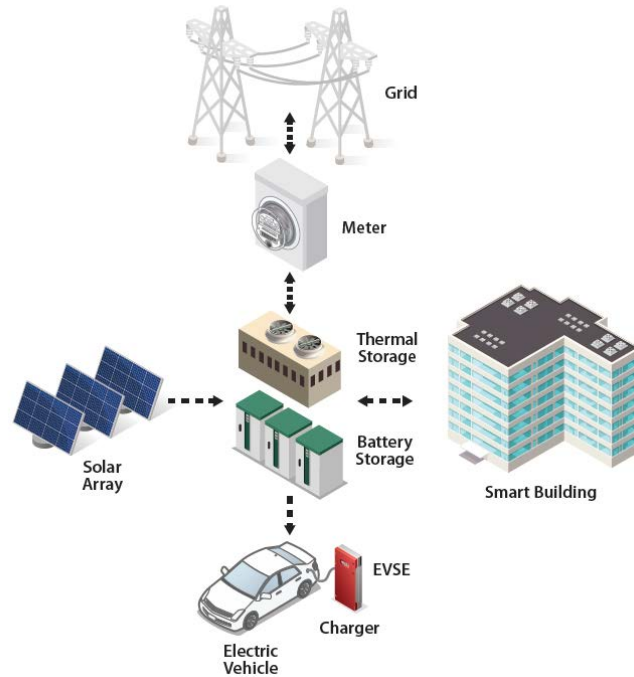
Figure 1. Overview of BTMS relevance.

BTMS Analysis : Inputs and Outputs of Model

National Renewable Energy Lab (NREL)
Margaret Mann, Madeline Gilleran, Feitau Kung, Matt Mitchell, Darice Guittet, Eric Bonnema, Jason Woods, Chad Hunter

Background

The Behind-the-Meter-Storage (BTMS) Analysis project is funded by the Buildings Technologies Office (BTO), the Vehicle Technologies Office (VTO), and the Solar Energy Technologies Office (SETO) within the Department of Energy's (DOE) Office of Energy Efficiency and Renewable Energy (EERE). The mission of EERE is to create and sustain American leadership in the transition to a global clean energy economy. Its vision is a strong and prosperous America powered by clean, affordable, and secure energy www.energy.gov/eere). Increasing adoption of electric vehicles (EV), solar photovoltaic (PV), battery and thermal storage, and energy-efficient buildinglif technologies is expected to have significant impact on energy use and domestic manufacturing. While each of these technologies can make contributions to the U.S. economy, integrating them in ways that optimize cost and energy flows for varying energy demand and climate conditions across the country can lead to multiplicative positive impacts.

BTMS research is targeted at developing innovative energy storage technology specifically optimized for stationary applications that will enable extreme fast charging of EVs, allow for enhanced grid interactive energy efficient buildings coupled with photovoltaic resources, while minimizing grid impacts.

EV adoption is expected to grow significantly over the coming years, and could have a significant, and potentially negative effect on grid infrastructure. Additionally, the rapid penetration of solar PV generation installed on buildings is leading to new challenges for the electric grid. In response to the potentially large and irregular demand from EVs, along with changing load profiles from buildings with on-site generation, utilities are evaluating multiple options for managing dynamic loads, including time-of-use pricing, demand charges, battery storage, and curtailment of variable generation. Buildings, as well as commercial, public, and workplace EV charging operations, can use energy storage (e.g., batteries, thermal energy storage, etc.) coupled with on-site generation to manage energy costs as well as provide resiliency and reliability for EV charging and building energy loads.

The key question in this project is the following: what are the optimal system designs and energy flows for thermal and electrochemical energy storage systems at sites with on-site photovoltaic (PV) generation and electric vehicle (EV) charging, and how do solutions vary with climate, building type, and utility rate structure?

The primary objective function for most analyses in this project will be the Levelized Cost of Charging, or LCOC. This metric, measured in cents/kWh, is the minimum price that EV station owners would need to charge users in order to "break even", or to pay back all capital and operating expenses over the lifetime of the system. A standardized discounted cash flow rate of return (DCFROR) analysis methodology is being utilized to calculate LCOC.

A high-level schematic depicting the various behind-the-meter systems, including stationary battery, solar PV, electric vehicle supply equipment (EVSE), and thermal energy storage (TES), can be seen in Figure 1.
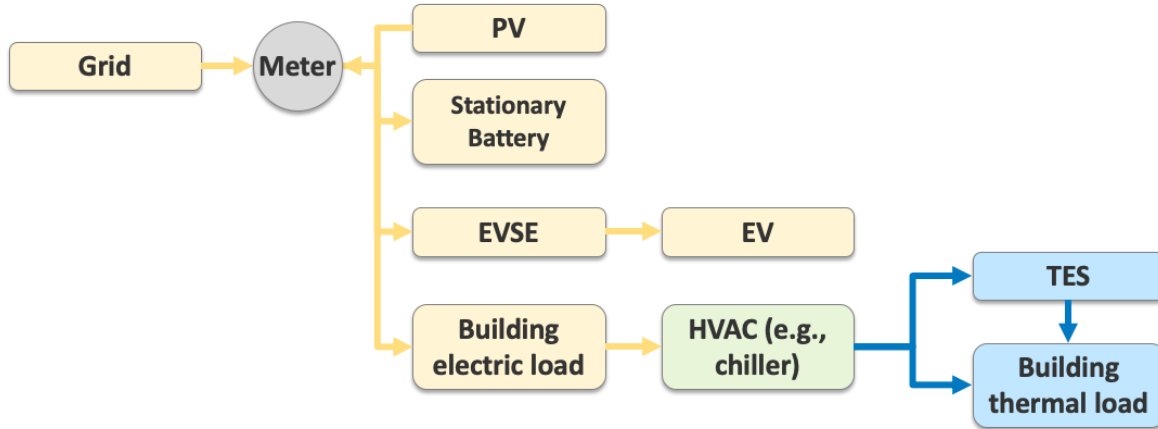
Figure 1. Schematic Depicting the Default Combination of Technologies for BTMS Analysis

To complete this analysis, the BTMS Analysis team is developing a multitool simulation platform called EnStore, which will be able to capture performance characteristics and interactions between disparate technologies with high fidelity. _In researching existing tools used in this space, the team concluded that no one existing tool could complete the multisystem, detailed analysis required for this project, but rather, a combination of several existing tools would be necessary._ This project will leverage the following tools: the REopt[TM] energy system optimization tool (Cutler et al. 2017), System Advisor Model (SAM) (Blair et al. 2018), Electric Vehicle Infrastructure Projection Tool (EVI-Pro) (Wood et al. 2018), the EnergyPlus[TM] building simulation engine (DOE 2019a), the OpenStudio® suite of supporting building simulation applications (DOE 2019b), and the Utility Rate Database (URDB) (DOE 2019c).

This report, submitted as Quarterly Milestone 1, will detail the main categories of inputs and outputs for the EnStore simulation platform. It will also describe related near-term improvements to existing tools that are expected to improve the capabilities of EnStore.

EnStore Model Process Flows

For any given application of EnStore, the simulation process can be divided into five major stages as shown in Figure 2. In the "Pre-Processing" stage, the team will prepare the inputs required to initiate an EnStore simulation. The next three stages, "Seeding," "Exploration," and "Reporting," include processes managed and executed by EnStore code. In the "Post-Processing" stage, the team will use output files created by EnStore to answer research questions for the associated application.

EnStore

Pre-Process	Seed	Explore	Report	Post-Process
• Generate the baseline building load profile. • Generate the electric vehicle charging station load profile. • Specify system costs, weather data, utility rate tariff, etc.	• Use **REopt** to limit the initial parameter space with simplified models and idealized controls. • Suggest initial sizes for stationary battery and solar PV.	• Model system and component variations with greater fidelity. • Use **OpenStudio/ EnergyPlus** for building loads, thermal storage, and supervisory controls; **SAM** for stationary batteries. • Vary selected parameters to explore impact on LCOC.	• Store key system characteristics, e.g., stationary battery, solar PV, and thermal storage sizes and corresponding LCOC. • Provide time-series outputs for post-processing.	• Analyze which parameter variations yield the lowest LCOC. • Analyze sensitivity of results to key input parameter values. • **Answer research questions.**

Figure 2. Major stages of the multitool workflow

In the Pre-Processing Stage, to generate inputs required for EnStore, the team plans to use a combination of tools, including the following:

- The team will use OpenStudio and EnergyPlus to generate a baseline building model that will be modified later in the Exploration Stage.
- These same building model may also be used to generate a load profile for use by REopt in the Seeding Stage. Alternatively, for some applications, the load profile for REopt may be generated using meter data or a combination of meter and model data.
- The team will use EVI-Pro and a DC Fast Charge (DCFC) model (created in the preceding FY19 project and completed in the first quarter of this FY20 project) to generate an EVSE load profile.
- Stationary battery cost inputs will be informed by the use of BatPaC, a source of battery cost estimates that are dependent on battery chemistry, as well as market-relevant updates.

The team will combine these and other inputs into a set of standardized input files prior to each EnStore simulation. The team will then use these files to indicate which system parameters will be variable or fixed for a given application.

In the Seeding Stage, EnStore will use REopt to calculate preliminary sizes for the stationary battery system and PV system (unless these sizes are fixed and known in advance for a particular application). The REopt-generated system sizes will be considered preliminary because REopt uses a mixed-integer linear programming (MILP) approach to calculate an absolute minimum value for cost optimization problems, and the MILP approach requires simplified, linearized models. This stage also omits physical details that can affect the accuracy of electrical and thermal load profiles and storage system performance. However, these simplifications can be useful at this stage for enabling relatively rapid calculation of preliminary system sizes, which can then be permutated and explored with more detailed models in the next stage of simulation.

The Exploration Stage will use higher-fidelity, physics-based models of load, generation, and storage systems to increase the accuracy of electrical power and heat transfer calculations. At this stage, EnStore will use OpenStudio, EnergyPlus, and SAM to examine how inclusion of more detailed component performance characteristics and system interactions can affect design optimization results. EnergyPlus will enable the team to capture a variety of critical electrical and thermal system interactions, such as the interactions between TES systems, space conditioning systems, internal gains (e.g., occupants, lighting, plug loads, process loads),

internal mass objects, construction elements, exterior conditions, operational schedules, and control systems. OpenStudio will make it easier to modify EnergyPlus models in a replicable manner. SAM will enable the team to compare solutions for stationary battery designs with different component-level characteristics, such as voltage vs. depth-of-discharge curves, temperature dependencies, calendar life models, and cycle life models. It will also allow exploration and permutation of system-level inputs, such as battery replacement conditions and dispatch algorithms. To enable co-simulation and supervisory control of key component models, EnergyPlus will call the SAM battery model at each simulation timestep via an EnergyPlus feature called Python EMS and a SAM Python module called PySAM.

For any given application of EnStore, user inputs will determine the number of REopt simulations required in the Seeding Stage as well as the number of OpenStudio/EnergyPlus/SAM simulations required in the Exploration Stage. The required number of REopt simulations will depend on the number of unique sets of REopt inputs included in a particular application. For example, if a particular case study includes two different EVSE profiles and all other inputs are fixed, the study will require two REopt simulations in the Seeding Stage.

In the Exploration Stage, EnStore will typically translate each REopt result into multiple OpenStudio/EnergyPlus/SAM simulations that will be used for parametric analysis. The total number of OpenStudio/EnergyPlus/SAM simulations will depend on the number of variable parameters that were selected by the user for a given application. In addition to a user-specified number of system size permutations, other variable parameters may include cost assumptions, energy storage component properties, building characteristics, control assumptions, and other inputs to Exploration Stage models.

Once the simulations are complete, EnStore will execute the Reporting Stage. At this point, EnStore will save select output files from previous stages and calculate additional output values. Time-series outputs will include power (kW) from grid to battery, grid to building, grid to EV charging station, solar PV to grid, solar PV to battery, etc. These values will be used alongside capital and operations and maintenance (O&M) costs in the PySAM UtilityRate5 and CashLoan modules to compute LCOC and/or net present value (NPV). These financial calculations utilize standardized methodologies known as discounted cash flow rate of return (DCFROR); further information on the approach can be found in most engineering and finance textbooks, with a good overview provided in Short, et al (1995).

Finally, in the Post-Processing Stage, the team will compare simulation results to identify the case with the lowest LCOC and/or NPV for a given study. The team may use additional scripts to further synthesize and analyze results to answer more specific research questions for the BTMS Analysis project. A more detailed process flow diagram for pre-processing, EnStore, and post-processing is shown in Figure 3.
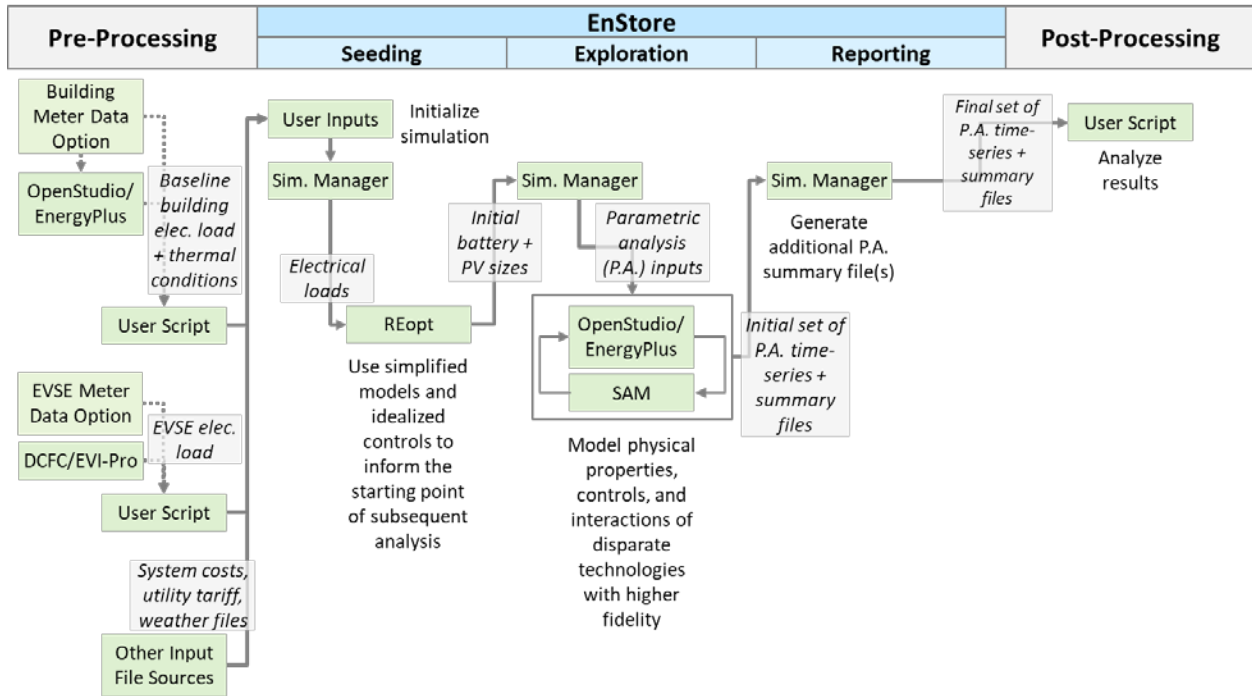
Figure 3. Draft model architecture details, including data exchanged between tools and stages

EnStore Model Inputs and Outputs

Certain categories of data are necessary to run EnStore. These include component system costs (e.g., battery installed cost per kW), utility rate tariff information, baseline building models, building load time-series profiles, EVSE load time-series profiles, and weather information (e.g., an .epw file).

These inputs collectively include data that are either required for specific tools used within EnStore (e.g., REopt, SAM, OpenStudio/EnergyPlus) or required for higher-level EnStore operations. EnStore will pass specific inputs to constituent tools as required.

EnStore Inputs and Outputs

The inputs and outputs of the EnStore simulation platform can be seen in Table 1 and Table 2.

<table>
<tr><td colspan="2" align="center">○   Table 1. Main Input Categories for EnStore</td></tr>
<tr><th>Input Category</th><th>Description</th></tr>
<tr><td>System Costs</td><td>Solar PV installed cost per kW, solar PV O&M cost per kW, battery installed cost per kW, battery installed cost per kWh, TES cost, EVSE capital and O&M costs, interconnection cost</td></tr>
<tr><td>Electric Utility Rate Tariffs</td><td>URDB label or custom rate tariff information</td></tr>
<tr><td>Net Metering Assumptions</td><td>Presence/absence of net metering; net metering rules if applicable</td></tr>
<tr><td>Building Loads</td><td>Baseline building model and load profile generated by OpenStudio in pre-processing for select building</td></tr>
</table>

	types, including retail big-box grocery store, commerical office building, fleet vehicle depot and operations facility, multifamily residential, and standalone EV charging station
EVSE Loads	Generated using EVI-Pro and DCFC Model with various demand scenarios
Weather Data	Typical Meteorological Year (TMY) (NSRDB) or Actual Meterological Year (AMY) data, saved in standard EnergyPlus format (.epw file)
Financial Information	Discount rate, tax incentives, etc.
Component-level Details	For stationary battery: battery chemistry, configuration, performance specifications, and control parameters, including max. and min. allowable SOC; For TES: TES type, configuration, and performance specifications; For solar PV: PV type, configuration, and performance specifications
Dispatch Control Logic	Supervisory dispatch control logic for dispatching stationary battery and TES
Power Electronics and Balance of Plant (BOP) Information	For example, AC-coupled system vs. DC-coupled system
Ownership Model	Whether system owner has purchased all technology assets (solar PV, stationary battery, TES, EVSE) or a subset of these
Stationary Battery Conditioning	Cooling/heating system assumptions, whether battery is placed inside or outside the building
Analysis Period	For example, 1 year vs. 20 years

o **Table 2. Main Output Categories for EnStore**

Output Category	Description
Financial Metrics	LCOC and NPV
Technology System Sizes	Solar PV kW, stationary battery kW and kWh, TES size
Time-series Data	Solar PV production, stationary battery charge/discharge rates; power from solar PV to grid, solar PV to EVSE, stationary battery to EVSE, grid to building, grid to EVSE, etc.; other system and subsystem loads and conditions

Inputs and Outputs for Other Tools in the BTMS Analysis Workflow

Generating Electric Vehicle Load Profiles

The team is using two models to generate EVSE load profiles: EVI-Pro and the DCFC model. EVI-Pro was developed by NREL in partnership with the California Energy Commission (CEC), and the DCFC model was developed by NREL and the University of Alabama (Ucer et al. 2018), with additional development in the preceding FY19 BTMS Analysis project in the first quarter of this FY20 project.

EVI-Pro utilizes EV market and real-world travel data to estimate future requirements for home, workplace, and public charging infrastructure. The team will use EVI-Pro simulation results to determine probability distribution functions for EV arrival time and initial state of charge (SOC). These can be adjusted for different applications, such as an EV fast charge station, a big-box retail grocery store, office buildings, and a multifamily residential building.

The DCFC model will use data generated from EVI-Pro as well as other data collected for the BTMS Analysis project. In the DCFC model, Monte Carlo simulations are carried out to predict the charging load and queuing time at a station. As explained by Ucer et al., "[during] each run, vehicle related parameters such as time of arrival, energy demand, initial SOC, etc. are randomly regenerated from the associated probability density functions (PDFs) [from EVI-Pro]. During the simulations, vehicles arrive at the corresponding stations, wait in the queue (if there is not any available port), are plugged in, and [are] then charged according to their charge acceptance curves. They depart after their energy demand is met, and a new vehicle from the queue is plugged into an available port." Inputs and outputs for the DCFC model are shown in Table 3 and Table 4.

o **Table 3. Main Input Categories for DCFC Model**

Input Category	Description
Probability Distribution Functions	Probability distribution functions for arrival time and initial SOC, initial SOC tied to kWh charged
Vehicle Battery Sizes	Battery sizes and ratio of battery sizes of vehicles charging at station (kWh)
Station Information	Station port capacity (kW) and number of ports at the station
Charging Event Frequency	Number of events per station per day
Battery Acceptance Curve Inputs	Battery chemistry needed to generate battery acceptance curve

o **Table 4. Main Output Category for DCFC Model**

Output Category	Description
EVSE Load Profile	Minute kW time-series load profile for single EV station for 28 days, post-processed for one year

Inputs and Outputs for REopt

As previously discussed, in the Seeding Stage of the EnStore workflow, the team will use REopt to calculate preliminary solar PV and stationary battery sizes using simplified, linearized models. The system sizes will be permutated later with more detailed models. Inputs and outputs required for using REopt in the EnStore workflow are summarized in Table 5 and Table 6. .
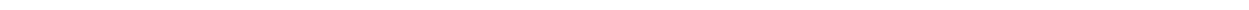
o   ### Table 5. Main Input Categories for REopt

Input Category	Description
Location	Latitude and longitude (REopt uses these to determine solar generation)
Electric Utility Rate Tariff Information	URDB label or custom rate tariff information
Cost Information	Solar PV installed cost per kW and O&M cost per kW; stationary battery installed cost per kW and installed cost per kWh; EVSE capital and O&M costs; interconnection cost
Detailed Component Information	Solar PV degradation percentage and existing kW; stationary battery replacement year, internal efficiency percentage, inverter efficiency percentage, inverter replacement year, max. kW, min. kW, initial SOC percentage, and min. SOC percentage
Load Profile	Aggregated building + EVSE load profile
Default Values	See REopt API documentation for details

o   ### Table 6. Main Output Category for REopt

Output Category	Description
Preliminary system sizes	Solar PV size (kW), stationary battery size (kW and kWh)

Inputs and Outputs for EnergyPlus and OpenStudio

EnergyPlus is a whole-building energy simulation engine, and OpenStudio is a suite of complementary tools that can expand EnergyPlus capabilities. As previously discussed, these tools will be used in both the Pre-Processing Stage and the Exploration Stage. Inputs and outputs required for using EnergyPlus and OpenStudio in the EnStore workflow are summarized in Table 7 and Table 8.

o   ### Table 7. Main Input Categories for EnergyPlus and OpenStudio

Input Category	Description
Baseline Building Model	Baseline building model (.idf or .osm file) with no solar PV, stationary battery, or TES. A different baseline building model will be created for each of the building types included in this project (retail big-box grocery store, commercial office building, fleet vehicle depot and operations facility, multi-family residential, and EV charging station)
Weather Data	Standard EnergyPlus format (.epw file)
Measures	In this context, "measures" are scripts for modifying building models in a replicable manner. EnStore inputs will include measures to add solar PV,

	stationary battery, and TES systems of various sizes.
Content for Python EMS	Depending on the application, examples may include: supervisory control logic for dispatching multiple energy storage systems; custom component models for novel TES technologies that differ from native EnergyPlus TES options; code for generating custom output variables.
Default Values	See the EnergyPlus Input Output Reference document for details

o **Table 8. Main Output Category for EnergyPlus and OpenStudio**

Output Category	Description

Time-series Data	Various time-series data will be used for post-processing, including the following:
	- Electrical power from:
	   o Grid to stationary battery
	   o Grid to EV charging station
	   o Grid to building
	   o Solar PV to grid (if applicable)
	   o Solar PV to building
	   o Solar PV to EV charging station
	   o Stationary battery to building
	   o Stationary battery to EV charging station
	   o Stationary battery to grid (if applicable)
	- Electrical input to TES systems
	- Thermal input to TES systems
	- Thermal output from TES systems
	- System losses
	- Other system and subsystem loads and conditions

Inputs and Outputs for the SAM StandAloneBattery Module

The SAM StandAloneBattery module is a detailed battery storage model that has detailed lifetime and degradation parameters, developed from work by Dey, et al. (March 2020). The SAM battery model will be instantiated within EnergyPlus to model battery capacity, output, losses, and life more accurately than would be possible with default EnergyPlus battery models.

o **Table 9. Main Input Categories for SAM Battery Module**

Input Category	Description
Stationary Battery Characteristics	- Battery size (kW and kWh) - Battery chemistry - Battery performance curves (e.g. voltage vs. depth-of-discharge curve)

	- Battery control parameters (e.g. max./min. allowable SOC) - Battery replacement assumptions (e.g., replace when capacity drops to 80% of original capacity)
Default Values	See PySAM Battery documentation for details

o **Table 10. Main Output Category for SAM Battery Module**

Output Category	Description
Time-series Data	Various time-series data will be used for post-processing, including the following: - Battery SOC - Battery kW charging/discharging rates - Battery temperature - Battery capacity fade

Inputs and Outputs for the SAM UtilityRate5 Module

UtilityRate5 PySAM module is a retail electricity bill calculator that uses the URDB and can apply net metering rules to determine monthly and annual electricity bills.

o **Table 11. Main Input Categories for SAM UtilityRate5 Module**

Input Category	Description
Time-series Data	- Electricity received from the grid - Exported surplus solar generation (for net metering)
Net Metering Assumptions	Presence/absence of net metering; net metering rules if applicable
Default Values	See PySAM Utilityrate5 documentation for details

o **Table 12. Main Output Category for SAM UtilityRate5 Module**

Output Category	Description
Electricity Bill	Monthly electricity bill

Inputs and Outputs for the SAM Cashloan Module

The Cashloan PySAM module is a financial model for residential and commercial behind-the-meter projects.

o **Table 13. Main Input Categories for SAM Cashloan Module**

Input Category	Description
Monthly Electricity Bill	From UtilityRate5 Module
Costs	Aggregated capital costs, aggregated additional O&M costs

Financial Information	Discount rate
Default Values	See [PySAM Cashloan documentation](#) for details

○   **Table 14. Main Output Category for SAM Cashloan Module**

Output Category	Description
NPV	Will be used to compute LCOC

Related Upgrades to Existing Modeling Tools

The BTMS Analysis team has engaged the development teams of related tools to understand their existing features and identify opportunities to leverage new features that will be completed soon enough to benefit this project. In particular, two upcoming features will be highly beneficial to the EnStore workflow:

- Python EMS is a new feature under development by the EnergyPlus team. In the EnStore workflow, Python EMS will facilitate development of custom component models and act as a communication bridge between EnergyPlus and PySAM. An early prototype of Python EMS is estimated to be available for internal testing by the BTMS Analysis team in the next quarter with development continuing in 2020.

- The SAM team is in the process of upgrading the PySAM battery module to enable Python EMS to call the SAM battery model at each simulation timestep. This is expected to improve transfer of battery state information between EnergyPlus and SAM models. An early version of this functionality is estimated to be available for internal testing by the BTMS Analysis team later in 2020.

Additionally, the BTMS Analysis team is coordinating with other personnel who are engaged in laboratory characterization of batteries for stationary applications. Staff will discuss how new laboratory data might inform the methods that will be applied by the BTMS Analysis team to model stationary battery variations later in this project. The team will revisit related inputs and modeling methods as more information becomes available.

Conclusions

The team has identified key sets of inputs and outputs that will be required to execute analyses with the EnStore multitool simulation platform. Input specifications are informed by requirements for EnStore-specific operations as well as requirements for constituent modeling tools, including REopt, SAM, OpenStudio, and EnergyPlus. Output specifications are informed by anticipated post-processing efforts that will be required to answer research questions for the BTMS Analysis project. In upcoming months, the team will continue developing code for the EnStore simulation platform. As more functionality is completed, the team will revisit the multitool architecture and revise input and output formats as needed to improve the workflow.

References

Blair, N., N. DiOrio, J. Freeman, P. Gilman, S. Janzou, T. Neises, M. Wagner. 2018. *System Advisor Model (SAM) General Description (Version 2017.9.5).* Golden, CO: National Renewable Energy Laboratory (NREL). NREL/TP-6A20-70414. https://www.nrel.gov/docs/fy18osti/70414.pdf.

Cutler, D., D. Olis, E. Elgqvist, X. Li, N. Laws, N. DiOrio, A. Walker, K. Anderson. 2017. *REopt: A Platform for Energy System Integration and Optimization.* Golden, CO: National Renewable Energy Laboratory (NREL). NREL Technical Report No. NREL/TP-7A40-70022. https://www.nrel.gov/docs/fy17osti/70022.pdf.

Dey, Satadru, Ying Shi, Kandler Smith, Andrew M. Colclasure, and Xuemin Li. (March 2020). "From Battery Cell to Electrodes: Real-Time Estimation of Charge and Health of Individual Battery Electrodes." IEEE Transactions on Industrial Electronics 67, no. 3: 2167–75. https://doi.org/10.1109/TIE.2019.2907514.

DOE (U.S. Department of Energy). 2019a. "EnergyPlus." https://www.energyplus.net.

DOE (U.S. Department of Energy). 2019b. "OpenStudio." https://www.openstudio.net.

DOE (U.S. Department of Energy). 2019c. "Utility Rate Database." https://openei.org/wiki/Utility_Rate_Database.

Short, W., D. J. Packey, T. Holt. 1995. "Manual for the Economic Evaluation of Energy Efficiency and Renewable Energy Technologie." *NREL Technical Report.* https://www.nrel.gov/docs/legosti/old/5173.pdf

Ucer, E., M. Kisacikoglu, F. Erden, A. Meintz, C. Rames. 2018. "Development of a DC Fast Charging Station Model for use with EV Infrastructure Projection Tool." *2018 IEEE Transportation Electrification Conference and Expo (ITEC)*: 904-909. https://doi.org/10.1109/ITEC.2018.8450158.

Wood, E., C. Rames, M. Muratori. 2018. "New EVSE Analytical Tools/Models: Electric Vehicle Infrastructure Projection Tool (EVI-Pro)." Golden, CO: National Renewable Energy Laboratory (NREL). NREL Presentation No. NREL/PR-5400-70831. https://www.nrel.gov/docs/fy18osti/70831.pdf.

BTMS Testing

Contributors: INL, SNL

Background

Life testing continues for a few selected commercial lithium-ion cell types, to probe their performance relative to early BMTS life goals. The status of this testing is presented and discussed, along with planned testing activities and procedure development.

Results

INL Testing

Graphite/NMC622 cells reached EOL, having lost 25% of their BOL capacity after 952 0.5C/0.5C full-depth cycles at 30°C, shown in figure 1. NMC622 cathodes have been shown in literature to trade cycling stability for energy density, and these commercial cells seem to be no exception: previous Graphite/NMC cells with lower Ni content have reached 5,000 cycles before EOL, though at slightly lower rates. Accordingly, the cycle life performance of these cells, as a benchmark for high-energy-density EV cells, should not be used to judge the cycle-life capability of graphite anodes in other systems. Another cell of the same type was cycled shallowly, and lost capacity at a similar rate, on an energy throughput basis, until 15% of its BOL capacity had faded. After that point, the shallowly cycled cell showed a decreased capacity loss rate as shown in figure 2.
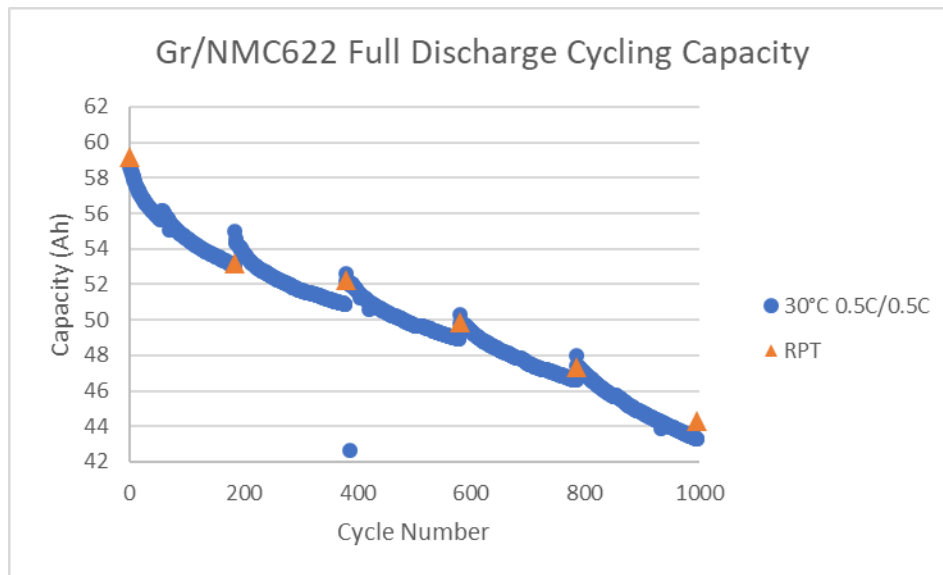
Figure 1. Graphite/NMC622 0.5C/05C cycle life capacity at 30°C
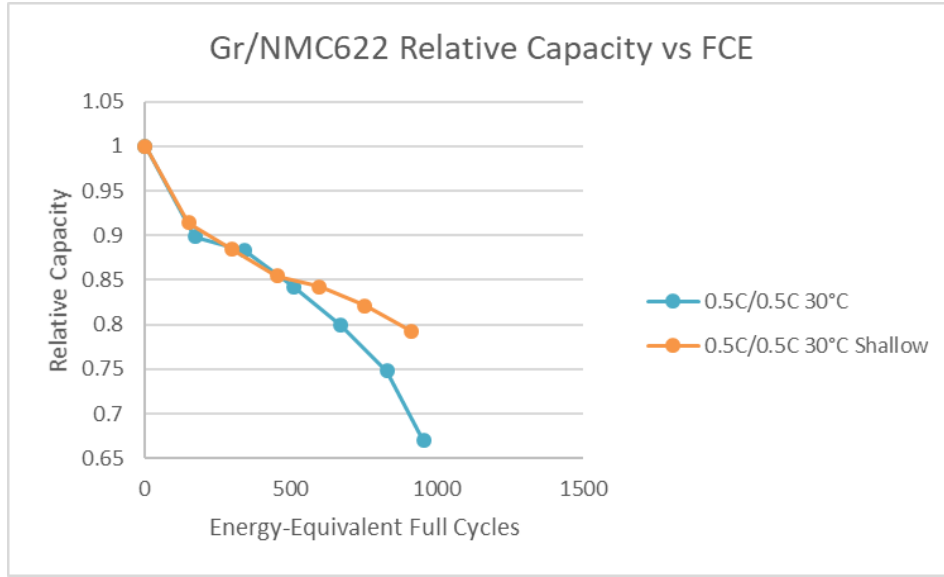
Figure 2. Graphite/NMC622 0.5C/05C full-depth and shallow cycle life capacity loss at 30°C

LTO/NMC cells optimized for long cycle life, but having a significantly lower specific energy, continue cycle and calendar aging using accelerating conditions with very little capacity loss observed, as shown in figure 3. Manufacturer literature on these cells suggests 80% capacity retention after 60,000 1C/1C cycles at 30°C, and extrapolation of the latest reference capacity loss points from the most accelerated aging condition, while not a prediction having any certainty, suggests that it is plausible these cells could cycle past the BTMS goal of 20,000 cycles, even at elevated temperature and rate, as shown in figure 4. Visual observation of these cells shows no excessive gassing to-date.
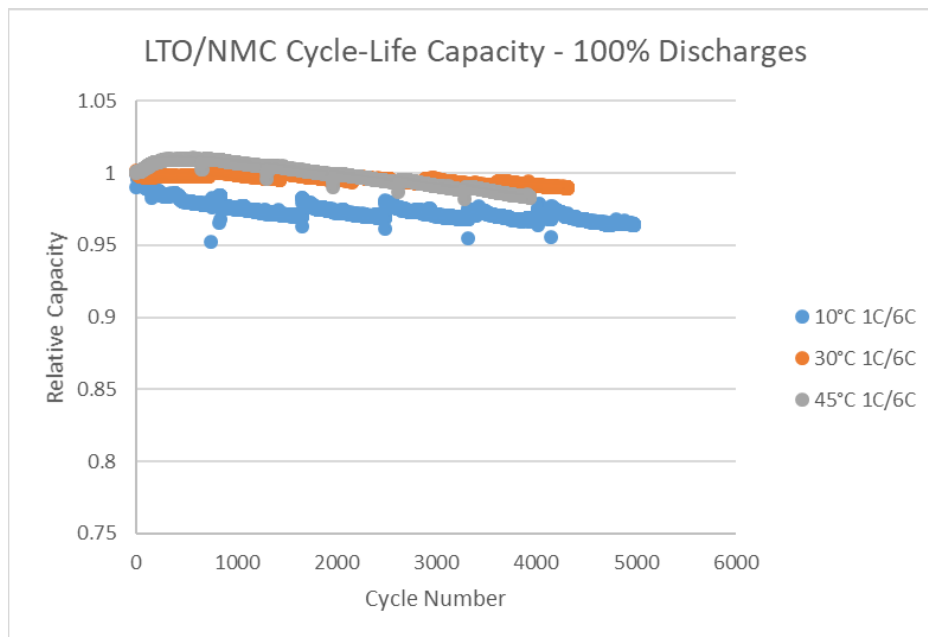
Figure 3. LTO/NMC 1C/6C full-depth cycle life capacity loss at 10, 30, and 45°C
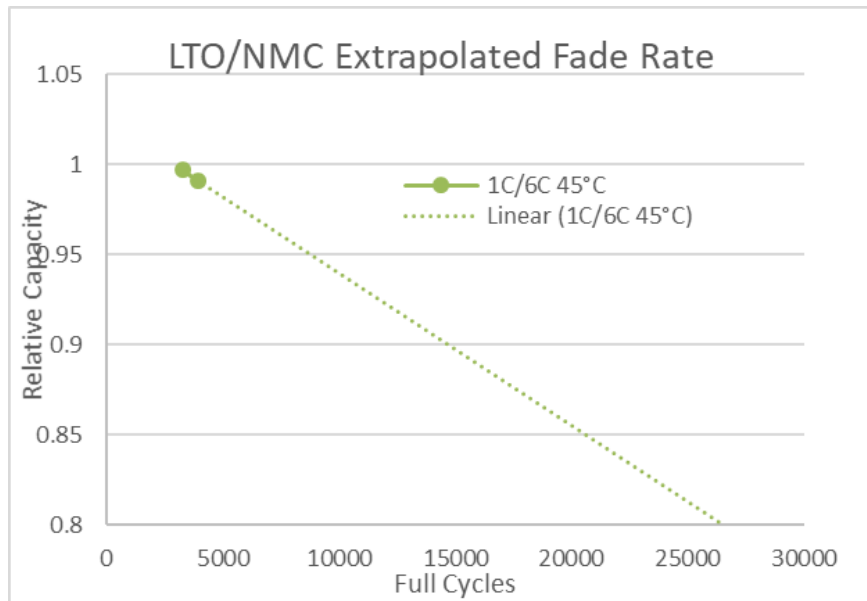
Figure 4. Extrapolation of RPT5 to RPT6 fade rate for LTO/NMC cells cycled at 1C/6C at 45°C

SNL Testing

Two different cell constructions are currently being investigated for the LFP/Graphite system. In some cases, the cells reached the target 1000 cycles and in other conditions they are close to 1000 cycles. The effects of this cycling on the capacity fade of the cells can be observed in figure 5.
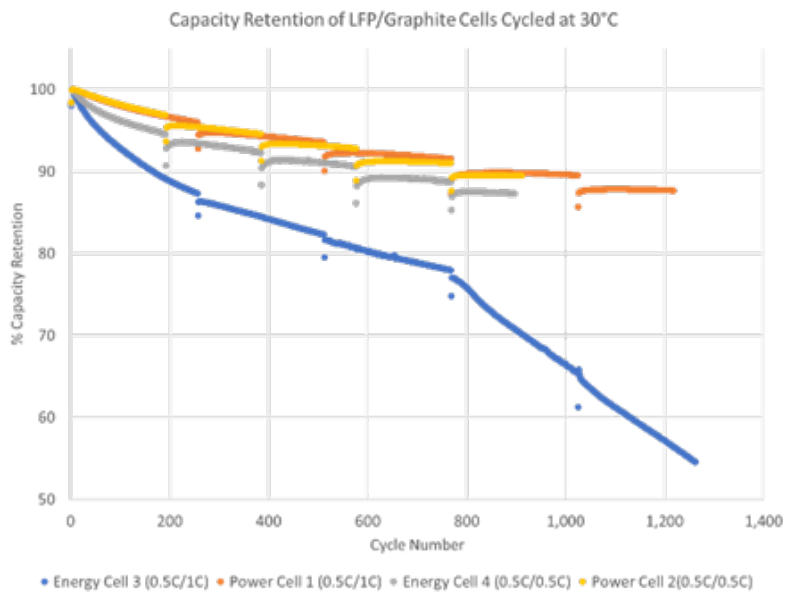
Figure 5. LFP/Graphite Cycling results

Results show that on average the power cells have lost ~13% while the energy cells have lost close to ~50% in the worst case. It is difficult to say of the ~50% loss in the energy cell is representative without additional cells to provide statistics. These results suggest that if similar decay rates persist, the cells cannot meet the 10000-cycle target as they will have run out of usable capacity. Differences in the state of health testing of these cells can also be observed as demonstrated in figure 6.
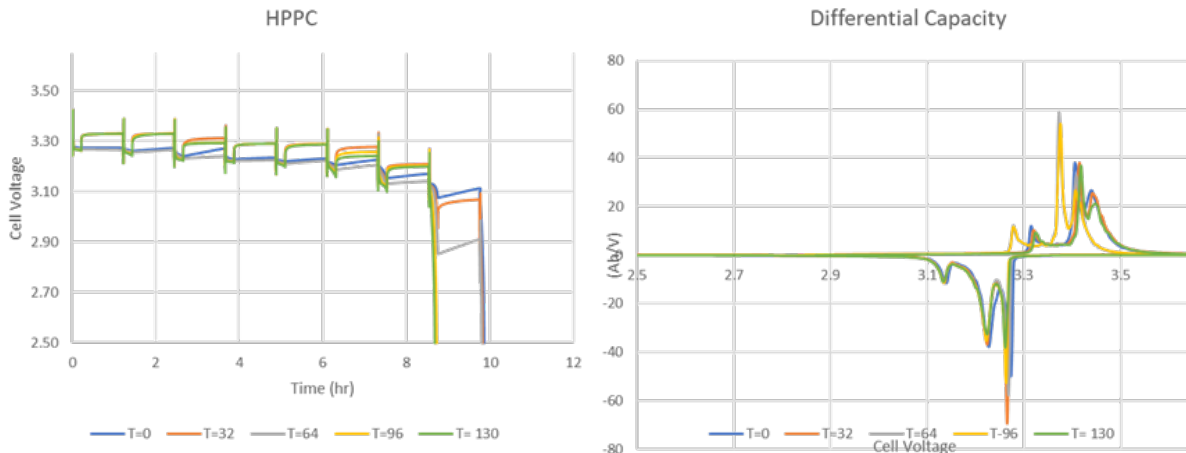
Figure 6: Power Cell 1 State of Health Testing of LFP/Graphite Cells

HPPC results show that as the cell continues to cycle, it loses its ability to deliver power at low states of charge which suggest that these cells will fail to meet the power demand required at end of life before the 10000-cycle target lifetime. The differential capacity results suggest that the loss of performance is most likely attributed to changes in the graphite anode with some contributions from cathode losses. This is a known problem. Graphite is known to degrade from extensive cycling.

Upcoming Testing

Orders have been placed for Toshiba LTO/LMO cells, and ZAF Ni Zn cells. The LTO/LMO is advertised to have very long cycle life, and the nickel zinc cells are touted as low cost and extremely recyclable, though cycle life is not expected to approach the BTMS goal. Both types of cells are critical material free.

Performance Testing Protocol Development

The initial testing protocols developed and reported on were designed to test the fundamental limits of the available commercial chemistries, and to better understand the aging mechanisms present in these chemistries. With a good understanding of the limitations of the available chemistries, a new series of testing protocols are being developed to mimic potential use cases of a BTMS application. For these test protocols the "gas station" model was considered in which the BTMS system would supply the energy needed to charge EV without assistance from the grid and be charged by the grid during off-peak hours. In this use case the BTMS system would need to support 4 events of 350kW EV charges (BTMS discharge) throughout the day. A 12 hour cycle as opposed to a 24 was chosen to double the amount of cycles per day and keep the charge rates low enough to ensure no accelerated aging mechanisms were enabled. Three different scenarios were considered. The first entailed 4 XFC events spaced evenly throughout the day, the second had two XFC events back to back at the beginning and end of the day, the third had an XFC event at the beginning and end of the day with two back to back EV charging events in the middle of the day. These test scenarios are outline below in figure 7.
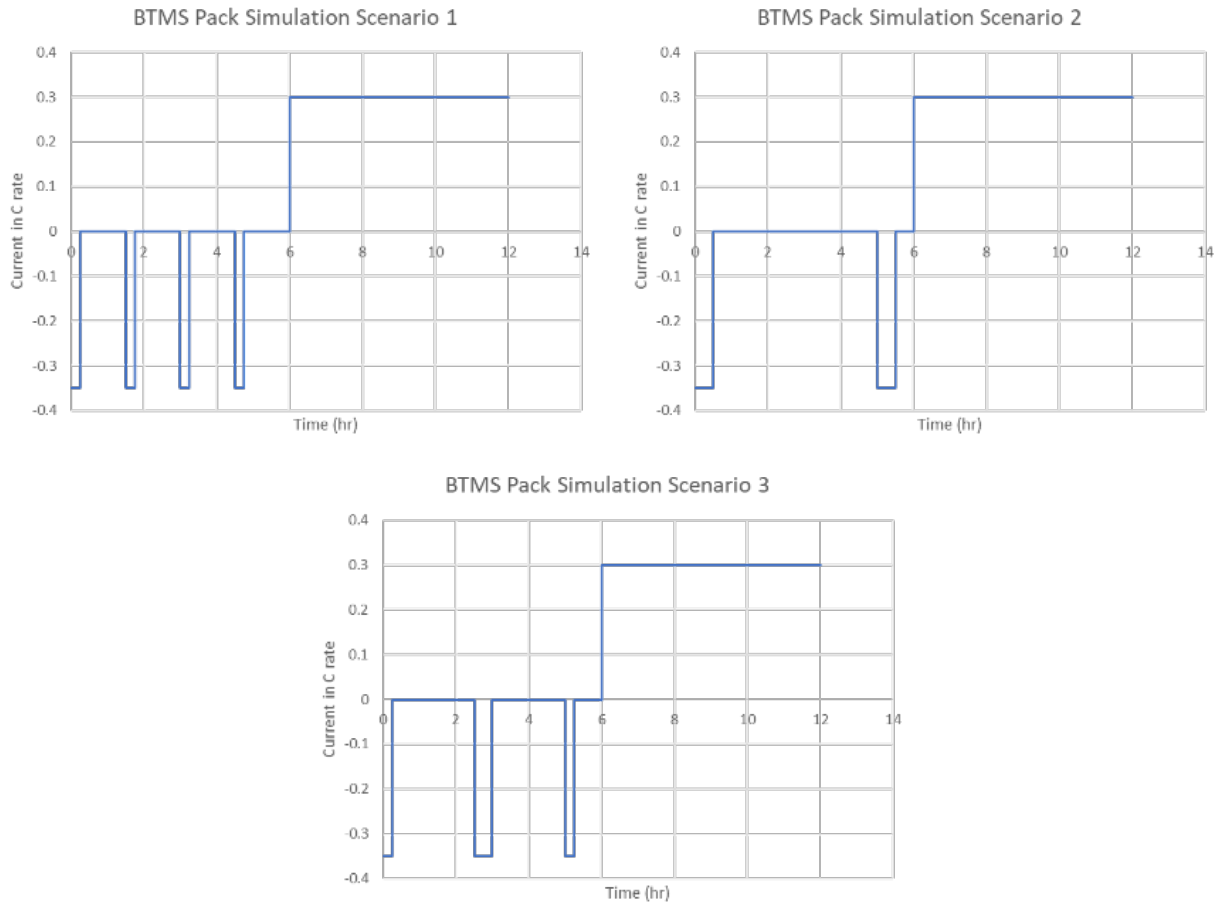
Figure 7. Test protocols mimicking potential use cases of BTMS powering an XFC station

Summary

Aging continues on commercial cells that began early in the program, not meeting the critical material free goal. New critical material free commercial cells are planned for testing and evaluation to serve as a benchmark for thick electrode, critical material free cells being designed specifically for BTMS applications.

Physics-based Machine Learning for Behind the Meter Storage

Idaho National Laboratory and National Renewable Energy Laboratory
Eric Dufek, Kandler Smith, Ross Kunz

Background

The development and deployment of batteries in new, diverse applications requires both that the batteries function in the necessary environment as well as a deep understanding of their performance, life and expected failure mechanisms. In the past the primary means to advance knowledge on performance and life was to test batteries for extended periods of time under a range of different scenarios. Testing of batteries in this manner can take upwards of a year to make reasonable estimations of life and to clearly identify failure modes and rates. The need to shorten the design and testing cycle if critical to bringing new battery chemistries and cell designs into emerging applications such as in stationary energy storage to support electric vehicle charging stations capable of extreme fast charging. Connection of physics-based life models and machine learning (ML) provides the opportunity to enable more robust assessment of battery aging, failure mechanism identification and understanding as new use case scenarios are proposed. The current project is focused on means to apply ML to enhance the estimation of life while also identifying key failure pathways. During the first portion of the project existing data sets will be used for both training and validation of ML approaches to better characterize expected battery life. The work also looks to link ML with existing physics-based life models at INL and NREL.

Results

Kokam Aging Analysis

The project objective is to reduce the time, cost and number of experiments needed to accurately quantify battery lifetime, supported by physics-based lifetime models and machine learning. A numerical description of model uncertainty is needed to support optimization of aging techniques for improved model accuracy with less test data.

In this quarter, the bootstrap resampling method was applied to quantify the uncertainty in NREL's battery life model. Bootstrap resampling simply generates new datasets by randomly resampling, with replacement, from the original dataset. Life model parameters can then be refit on the bootstrapped datasets to determine their uncertainty. A simple schematic demonstrating the bootstrap resampling technique is shown below:

Original dataset: Resampled datasets (with replacement):

$$x_0 = \begin{bmatrix} 1 \\ 2 \\ 3 \\ 4 \\ 5 \end{bmatrix} \quad \begin{matrix} \text{Bootstrap} \\ \text{resampling} \\ (n \text{ times}) \\ \rightarrow \end{matrix} \quad x_1 = \begin{bmatrix} 4 \\ 1 \\ 1 \\ 2 \\ 5 \end{bmatrix} \quad x_2 = \begin{bmatrix} 1 \\ 5 \\ 4 \\ 3 \\ 3 \end{bmatrix} \ldots \quad \ldots x_n = \begin{bmatrix} 2 \\ 4 \\ 1 \\ 3 \\ 1 \end{bmatrix}$$
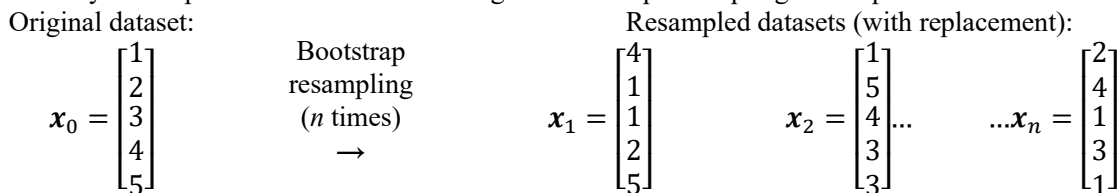
The dataset used for initial development of the bootstrap resampling technique is composed of cell testing results from eleven Kokam graphite/NMC 75-Ah lithium-ion batteries which were tested at varying temperatures, average states of charge, and cycling conditions [1]. These test results are then fit with reduced-order physics-based capacity fade and resistance growth models, accounting for several degradation pathways visible in the dataset. A table detailing the testing parameters and a figure showing the testing data and the fitted capacity fade model are shown in Table 1 and Figure 1, respectively.

| Test # | Cycling tests | | | | |
	Temperature	DOD	Dis./charge rate	Duty-cycle[a]	# of cells
1,2	23°C	80%	1C/1C	100%	2
3	30°C	100%	1C/1C	100%	1
4	30°C	80%	1C/1C	50%	1
6,7	0°C	80%	1C/0.3C	100%	2
9	45°C	80%	1C/1C	100%	1

| Test # | Storage tests | | |
	Temperature	SOC	# of cells
5	30°C	100%	1
8	45°C	65%	1
10	45°C	100%	1
11	55°C	100%	1

a.   Fraction of cycling time to total time

Table 15: Aging tests for Kokam 75-Ah cells [1].
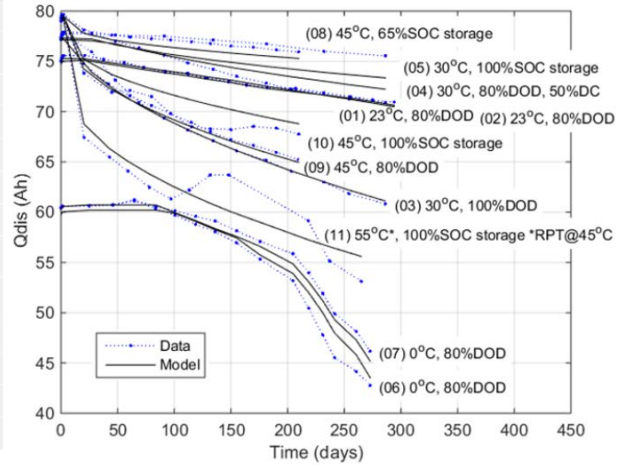
Figure 4: Kokam capacity fade model, incorporating positive electrode degradation, negative electrode degradation, and lithium loss mechanisms [1].

After bootstrap resampling to generate new datasets, the parameters of the capacity fade model are then individually refit on each dataset. Examples of parameters include the activation energy for lithium loss during storage, as modeled by an Arrhenius relationship, or the lithium-inventory capacity loss per cycle (at a reference temperature of 25°C), which is assumed to be linear. In total, there are 19 parameters in the Kokam capacity fade model. The goal of bootstrap resampling is to determine both the sensitivity of the capacity fade model to individual parameters as well as the distribution of parameters values across the resampled datasets. The parameter distributions can be later used to generate random parameter values, enabling a Monte-Carlo approach for quantifying lifetime-predictive uncertainty.

A simple way to quantify the sensitivity of the capacity fade model to each parameter is to observe the distribution of the overall fit quality across the resampled dataset for each parameter. This is shown in Figure 2 for parameters refit on 100 bootstrapped datasets. Fit quality is quantified by 'r^2 adjusted'. For reference, the r^2 adj. value of the overall capacity fade model is about 0.985. The 95% confidence interval of r^2 adj. for most parameters is similar, implying that the capacity fade model is not dominated by any one parameter. The mean r^2 adj. for some parameters appears slightly higher than the 'true' value of 0.985, suggesting that these parameter values could be better optimized.
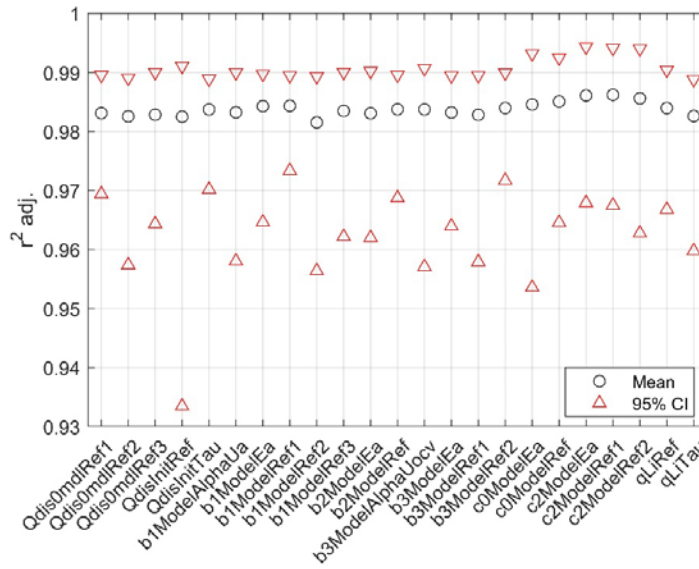
Figure 5: Variation of overall capacity fade model fit quality when parameters are refit over 100 bootstrapped datasets.

The effect of the number of bootstrapped samples on fit quality when refitting parameters is shown in Figure 3. The behavior is straightforward to explain; as the number bootstrapped datasets increase, the distribution of each parameter approaches its 'true' distribution, and the uncertainty value of each parameter will stabilize. Note that the total possible number of randomly resampled datasets is equal to $N!$, where N is the number of data points, but far fewer than $N!$ bootstrap samples need to be recorded before the uncertainty estimate stabilizes. Even at 100 samples, the mean fit quality is approaching the 'true' value of 0.985 for all parameters.
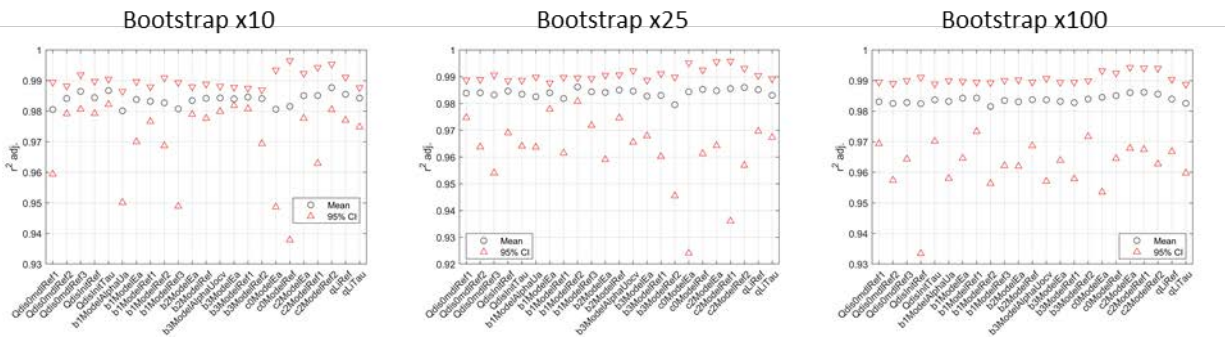
Figure 6: Variation of overall capacity fade model fit when parameters are refit over 10, 25, and 100 bootstrapped datasets.

The distributions of some of the bootstrapped parameter values are shown in Figure 4, as well as their mean, standard deviations, and estimated distribution. However, note that not all parameters appear to be normally distributed - some parameters are almost continuously distributed across their range, while others are distributed very asymmetrically with a long tail. A better way to fit arbitrary distributions is with the Kernel distribution, which are shown in Figure 5. Instead of fitting the mean of each parameter, the most probable value can be fit – if the distribution of the parameter is normal, these will be exactly equal. For distributions that are not well fit by a normal distribution, the most probable value is still similar to the mean from the normal distribution, but parameter values away from the mean are described more accurately. This is critically important for later Monte-Carlo simulations, where parameter values will be randomly drawn from these distributions.
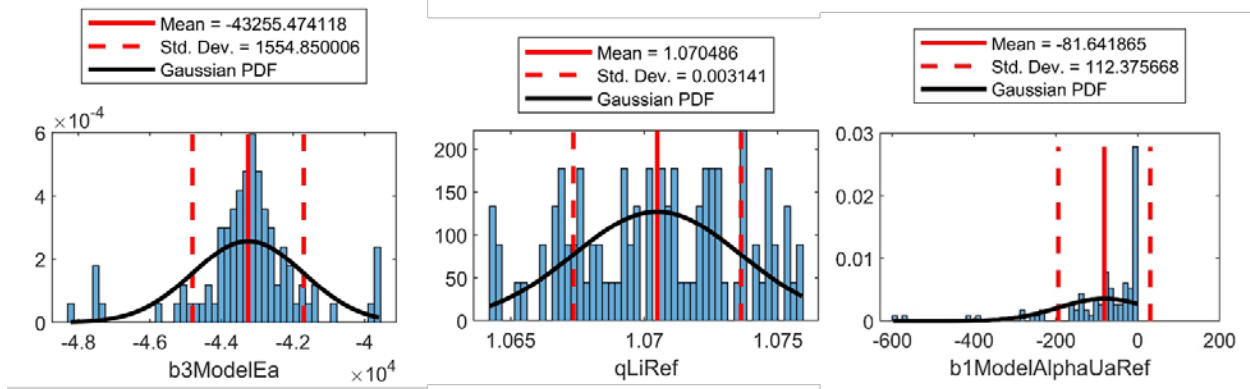
Figure 7: Example parameter distributions from bootstrap resampling 100 times. Distributions are fit assuming a gaussian distribution.
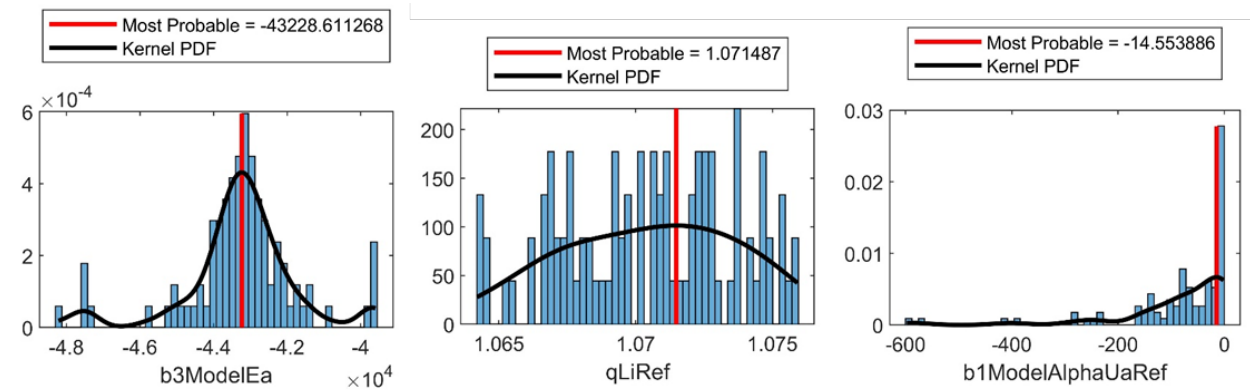
Figure 8: Example parameter distributions from bootstrap resampling 100 times. Distributions are fit assuming a Kernel distribution.

The capacity fade model recalculated using the parameter means and parameter 'most probable values' are compared with the original capacity fade model in Figure 6 below. Both methods of parameter estimation work well, but the Kernel distribution approach fits slightly better. This can clearly be seen by examining the 0°C cell data and predictions.
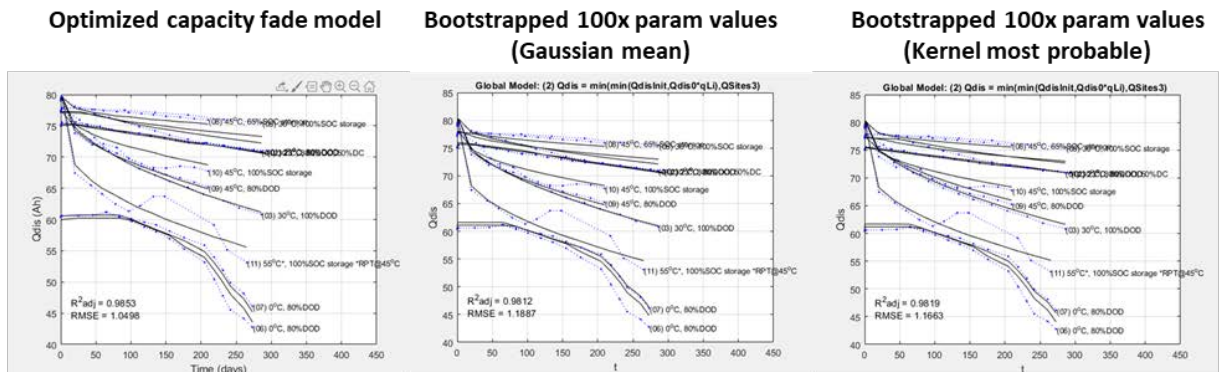
Figure 9: Optimized capacity fade model compared with capacity fade models calculated using parameter values from 100x bootstrapped parameter distributions.

The kernel distributions of each parameter can also be used to generate random parameter values for running Monte-Carlo simulations of the capacity fade model. These Monte-Carlo simulations can then be used to

create confidence intervals around the life model prediction. Figure 7 and Figure 8 below show initial results of this approach, using parameter distributions calculated by bootstrap resampling 1250 times, generating 300 sets of randomly sampled parameter values from these distributions, and then calculating the 95% confidence interval from the resulting capacity fade models. In Figures 7 and 8, the 'best fit' line is the original capacity fade model, and the 'updated params' line is the capacity fade model using the most probable parameter values from the bootstrap resampling stage. Figure 7 shows individual cells with different degradation patterns: the first cell shows degradation proportional to $t^{1/2}$, the second cell shows negative electrode site loss leading to a rapid drop off of capacity, and the third cell shows substantial beginning-of-life positive electrode 'break-in', causing a capacity increase, followed by almost linear degradation. It can be clearly seen that the uncertainty of the capacity fade model changes based on which of these mechanisms is dominating cell capacity loss, demonstrating how each mechanism has its own inherent uncertainty. Figure 8 shows the uncertainty windows for all the cells. Uncertainty is clearly highest for the cells tested at 0°C and 55°C.

Figure 10: Monte-Carlo simulation of the Kokam capacity fade model (individual cells plotted for comparison of degradation modes), calculated from 300 parameter sets that were randomly sampled from parameter distributions determined by bootstrap resampling 1250 times.
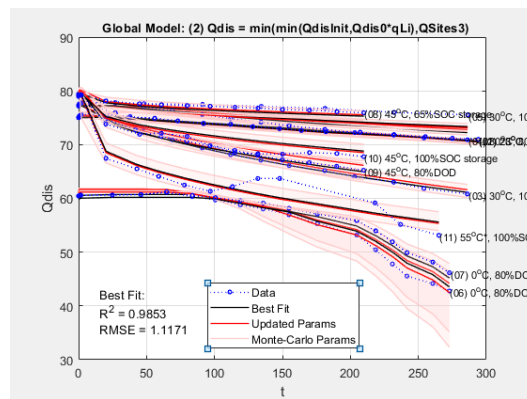
Figure 11: Monte-Carlo simulation of the Kokam capacity fade model, calculated from 300 parameter sets that were randomly sampled from parameter distributions determined by bootstrap resampling 1250 times.

These uncertainty windows can possibly be narrowed by changing the bootstrap resampling procedure to better reflect how the capacity fade model was actually fit to the data; the capacity fade model was originally built by selectively fitting specific degradation mechanisms to portions of the data that appear to behave by them (e.g., fitting the negative electrode site loss model to the 0°C cell data past 100 days, when cell capacity fade rate began to accelerate), while the bootstrap resampling procedure simply fits an individual parameter at a time across the entire data set.

Leaf Aging Analysis

In a continuation of activities which occurred to close FY19 the team further analyzed previously collected data related to aging of Nissan Leaf Cells [2]. When initially performed the aging data clearly identified aging trends using standard performance analysis methods, but the full analysis treated each condition as the average of multiple cells to draw general trends associated with different fast charging conditions as shown in Figure 9.
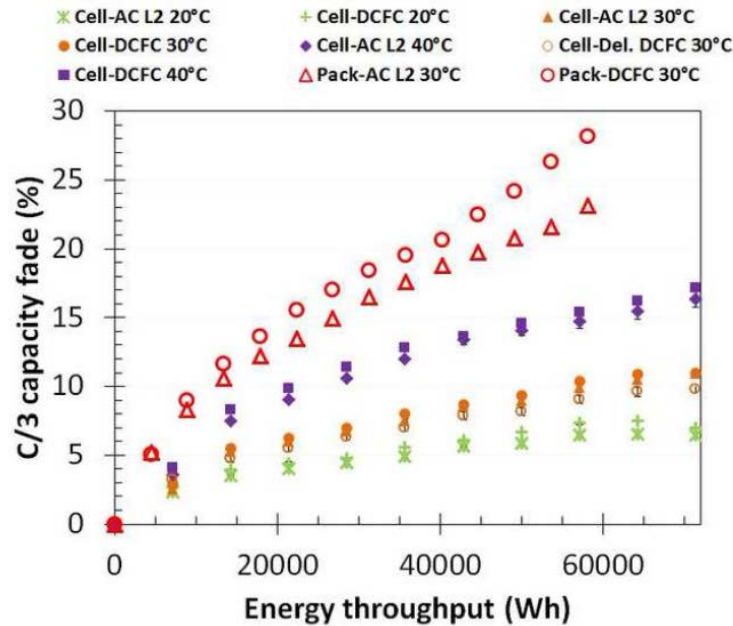
Figure 9: Capacity fade trades as a function of energy throughput for Nissan Leaf cells tested using a scaled AC level 2 or a DC Fast Charge charge profile. Data from Tanim et al [2].

Using the data in Figure 9 plus additional data that was not included in previous analysis which included combined AC Level 2 and DCFC in the same aging profile analysis was expanded using the ML architecture developed in Q1. The analysis was focused on two primary areas. First, using the data collected during both the charge and the discharge, the ability to accurately predict performance at a specified point in future time. The second focus area was on identifying and understanding variations within the original data points. Using time series outlier detection, outliers were identified from across the cycling domain for each of the cells as previously described. The data was then analyzed to look for clusters of cell performance and a cluster dendrogram was developed to group cells by similar performance as shown in Figure 10. As can be seen, the cell performance can be effectively clustered based on capacity fade. Using this input the earlier methods were refined to predict performance at RPT 9 (after 900 cycles). The initial prediction discussed in FY19 had an error of just over 1% when using the first 5 cycles of data. Following the time series dimension reduction this reduced to below 0.3% while also seeing a RMSE reduction to below 0.1.
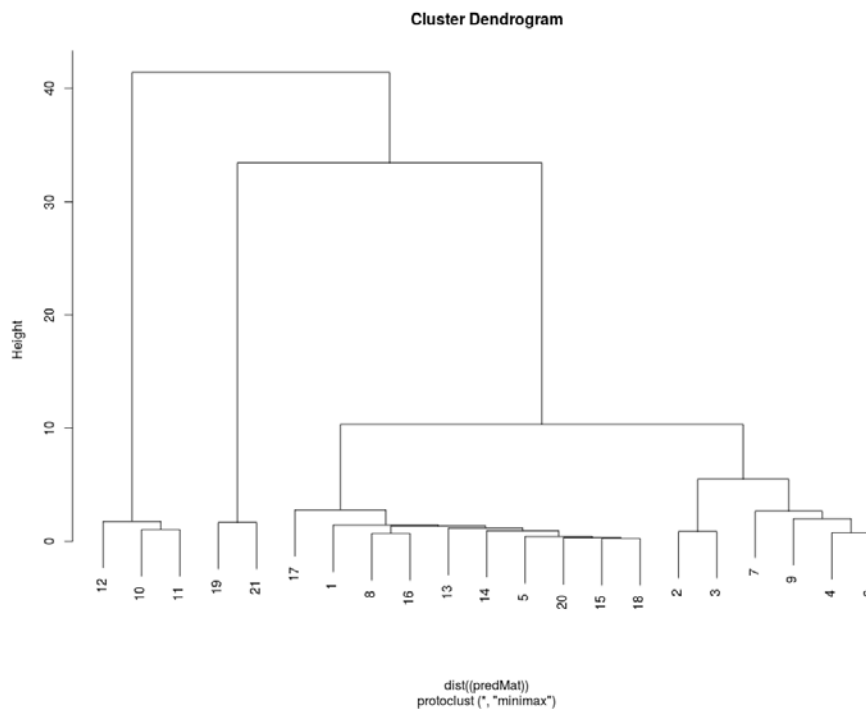
Figure 10: Cluster dendrogram showing similar performance of cells after the applications of time series outlier detection.

Project logistics and future aging studies

The team also developed future plans inline with the Q1 milestone for FY20 on a full design of experiment to support additional ML advancement. The DOE includes both cycle and calendar aging conditions for three state of charge conditions and three different temperatures. To facilitate additional conditions a reduced order design was adopted. The complete design includes a total of ~70 cells. Upon finalizing the design commercial off the shelf cells were procured to enable the start of testing during Q2 of FY20.

The team also worked to further enable data sharing and analysis through developing a plan to enable the use of shared software that will enable analysis and script development.

Conclusions

The team further developed ML methods during Q1. Bootstrap resampling of parameters combined with Monte-Carlo simulations of battery capacity fade has been initially demonstrated as a method for quantifying the uncertainty of NREL's battery capacity fade model. The bootstrap resampling procedure can be further improved to reduce the model uncertainty. Future work will extend the capacity fade model uncertainty quantification to simulations, and work to improve the resampling procedure to better reflect the original model fitting procedure. Robust analysis of outliers also showed distinct promise in reducing prediction error at defined locations for multiple charging and use protocols. A refined design of experiment was developed for future analysis needs and cells were procured to enable activities in Q2 and beyond.

References

[1] K. Smith, A. Saxon, M. Keyser, B. Lundstrom, Z. Cao, and A. Roc, "Life prediction model for grid-connected Li-ion battery energy storage system," *Proc. Am. Control Conf.*, pp. 4062–4068, August 2017.

[2] "Fast Charge Implications: Pack and Cell Comparison and Analysis" Tanvir R. Tanim, Matthew Shirk, Randy L. Bewley, Eric J. Dufek and Boryann Liaw, *J. Power Sources,* 381 (2018), 56-65

BTMS Materials Development

Yeyoung Ha, Sang-Don Han, Kyusung Park (NREL), Andrew Jansen (ANL)

Background

To meet the unique requirements for the Behind-the-Meter Storage (BTMS) systems – batteries capable of discharging at high power and charging at standard lower power rates, acting as a power reservoir to bridge to the grid and other on-site energy generation technologies – we are focusing on developing battery technologies with long cycle life (at least 8,000 cycles) and critical-material-free (e.g. Co-free cathodes) for stationary applications. $Li_4Ti_5O_{12}$ (LTO), which offers excellent safety and long cycle life as it operates around 1.55 V (vs. Li/Li$^+$) (eliminating potential Li dendrite formation) and exhibits minimal volume changes during lithium insertion/extraction,[1] is chosen as the anode and Mn-based cathodes ($LiMn_2O_4$, $LiNi_{0.5}Mn_{1.5}O_4$, and Li_2MnO_3-$LiMO_2$) are chosen as Co-free cathodes to be examined. While there have been reports on the LTO anode and Mn-based cathode cells in different electrolyte systems,[2] the studies were not targeted for the BTMS purpose. Thus, with the selected electrodes, we performed thorough examination of a variety of electrolytes focusing on their anodic (corrosion) stability and cycling performance at 45°C.

Results

To screen the liquid electrolytes for Mn-based cathodes ($LiMn_2O_4$, $LiNi_{0.5}Mn_{1.5}O_4$, and Li_2MnO_3-$LiMO_2$) and LTO anode chemistry, first we surveyed the literature and narrowed down Li salt and solvent candidates listed in Figure 1. Salts were chosen based on the following properties: (1) Lithium hexafluorophosphate ($LiPF_6$) and Lithium tetrafluoroborate ($LiBF_4$), which are known to successfully passivate Al current collector through the formation of AlF_3; (2) Lithium bis(trifluoromethanesulfonyl)imide (LiTFSI) and Lithium bis(fluorosulfonyl)imide (LiFSI), imide-based salts which exhibit good thermal stability and are less sensitive to moisture; and (3) Lithium trifluoromethanesulfonate (LiTf), Lithium acetate (LiOAc), and Lithium trifluoroacetate (LiOTFAc), lithium salts based on the conjugate bases of the acids.[3-4] Solvents were chosen based on the following properties: (1) Propylene carbonate (PC), which exhibits wide liquid range and high dielectric constant; (2) Fluoroethylene carbonate (FEC), another cyclic carbonate which may participate in the formation of beneficial solid-electrolyte interface (SEI) via incorporation of fluorine; and (3) Acetonitrile (ACN), Ethyl methyl sulfone (EMS), and Tetramethylene sulfone (TMS), which have been reported to have good anodic stability.[5-6] Mono-salt and -solvent combinations of these salts and solvents (1 M concentration) were examined.

Salt Candidates
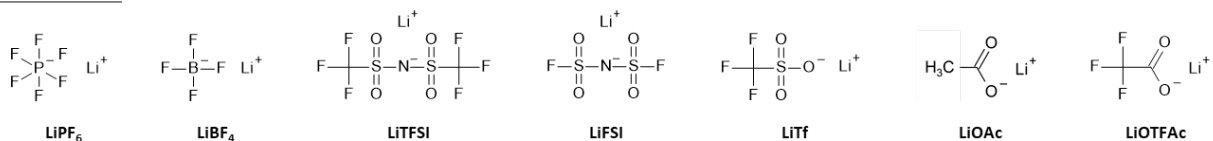
Solvent Candidates
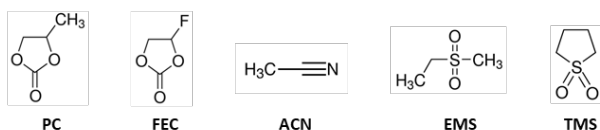
Figure 12. List of salts (Lithium hexafluorophosphate ($LiPF_6$), Lithium tetrafluoroborate ($LiBF_4$), Lithium bis(trifluoromethanesulfonyl)imide (LiTFSI), Lithium bis(fluorosulfonyl)imide (LiFSI), Lithium trifluoromethanesulfonate (LiTf), Lithium acetate (LiOAc), and Lithium trifluoroacetate (LiOTFAc)) and solvents (Propylene carbonate (PC), Fluoroethylene carbonate (FEC), Acetonitrile (ACN), Ethyl methyl sulfone (EMS), and Tetramethylene sulfone (TMS)) tested for the initial electrolyte screening.

Anodic stability test. As the initial screening process, the stability windows of electrolytes were tested in Al/Li coin cells using cyclic voltammetry because both the Mn-based cathodes and LTO anode use Al foil as the current collector. The cells were cycled between 1 and 5 V (vs. Li/Li$^+$) at 1 mV/s scan rate. All experiments were performed at room temperature. The second anodic (positive) scan for each electrolyte is presented in Figure 2. A lower current indicates that the electrolyte can successfully passivate the Al surface during the first cycle. The results for LiOAc are not shown as the salt did not dissolve in PC, FEC, and ACN, and showed chemical reactions with EMS and TMS and hence was not able to be tested. LiBF$_4$ in EMS, and LiOTFAc in EMS and TMS also showed chemical reactions between the salt and the solvent. Among the ones tested, LiPF$_6$, LiBF$_4$, and LiOTFAc exhibited a good anodic stability, indicating that using a fluorine-containing salt is effective in passivating Al surface via formation of AlF$_3$. With these salts, PC and FEC showed a better stability compared to ACN and sulfones. On the other hand, all imide-based salts (LiTFSI, LiFSI, and LiTf) had narrow stability windows.
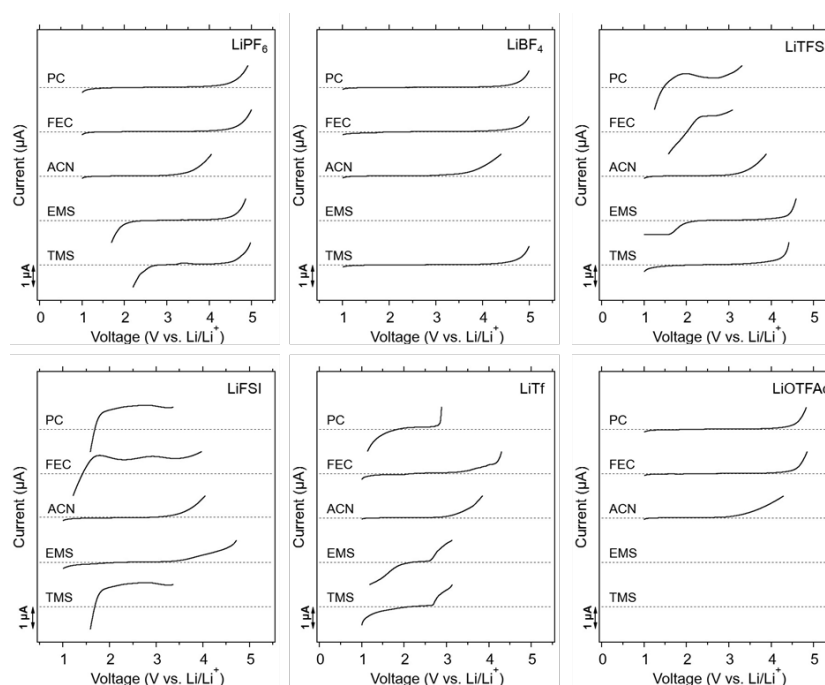
Figure 13. Electrochemical stability windows of electrolytes tested with Al/Li coin cells at room temperature. Al electrode was cycled between 1 and 5 V (vs. Li/Li$^+$) at 1 mV/s scan rate. The second anodic scan (1 V → 5 V) is presented as an indicative of determining the Al surface passivation. Electrolytes with LiBF$_4$ in EMS and LiOTFAc in EMS and TMS showed chemical reactions and could not be tested.

Half-cell test. Based on the anodic stability test results, three salts were selected to be examined in half-cells: LiPF$_6$ and LiBF$_4$, which showed good anodic stability; and LiTFSI, a representative of the imide-based salts which showed worse anodic stability than the other two salts. All five solvent systems (15 electrolytes in total) were tested. Three electrodes provided by CAMP Facility (LTO, LiMn$_2$O$_4$ (LMO), and LiNi$_{0.5}$Mn$_{1.5}$O$_4$ (LMNO)) were tested and their detailed information is given in Table 1. The half-cells were cycled at C/10 for 2 formation cycles and at 1C for 100 aging cycles. 1.0-2.5 V, 3.2-4.3 V, and 3.5-5.0 V cutoff voltages were used for LTO/Li, LMO/Li, and LMNO/Li cells, respectively. All cells were tested at 45°C. Surprisingly, the electrolytes showed the same trend in the cycle performance regardless of the electrodes tested (results not shown). To verify the effect of Li metal on the half-cell performance, Li/Li symmetric cells were tested in selected electrolytes: LiBF$_4$ and LiTFSI in PC and FEC. The symmetric cells were cycled by applying 2

mA/cm^2 during 1 h half-cycle. The current density and half-cycle time were chosen to match the areal capacity of the LTO/Li cells. In Figure 3, the cycle performance of LTO/Li and Li/Li cells are presented. First, looking at the LTO/Li cell results, FEC-based electrolytes showed a better capacity retention than the PC-based electrolytes with both LiBF$_4$ and LiTFSI salts. In particular, a rapid capacity decay was observed in the LiBF$_4$/PC electrolyte after ~20 cycles. This trend in the cycle performance, LiBF$_4$/PC << LiTFSI/PC < LiBF$_4$/FEC < LiTFSI/FEC, is clearly observed in the Li/Li cells as well, where the overpotential dramatically increases around ~20th cycle in LiBF$_4$/PC electrolyte, gradually increases in LiTFSI/PC, and remains relatively consistent in the FEC-based electrolytes. The performance of Li/Li symmetric cells directly correlate with the half-cell performance, indicating that half-cells cannot be used to obtain meaningful electrolyte screening data.

○ **Table-1: Electrodes Examined in this Report**

	Specifics
Li$_4$Ti$_5$O$_{12}$ (LTO)	- 87 wt% Samsung Li$_4$Ti$_5$O$_{12}$ + 5 wt% Timcal C45 + 8 wt% Kureha 9300 PVDF - Single side coating on 20 µm Al foil - Coating thickness 102 µm; Porosity 55.6 %; Loading 14.20 mg/cm^2; Density 1.38 g/cm^3
LiMn$_2$O$_4$ (LMO)	- 90 wt% Toda LiMn$_2$O$_4$ + 5 wt% Timcal C45 + 5 wt% Solvay 5130 PVDF - Single side coating on 20 µm Al foil - Coating thickness 76 µm; Porosity 33.5 %; Loading 18.86 mg/cm^2; Density 2.48 g/cm^3
LiNi$_{0.5}$Mn$_{1.5}$O$_4$ (LMNO)	- 84 wt% LiMn$_{1.5}$Ni$_{0.5}$O$_4$ + 8 wt% Timcal C45 + 8 wt% Solvey 5130 PVDF - Single side coating on 20 µm Al foil - Coating thickness 62 µm; Porosity 33.8 %; Loading 14.88 mg/cm^2; Density 2.40 g/cm^3
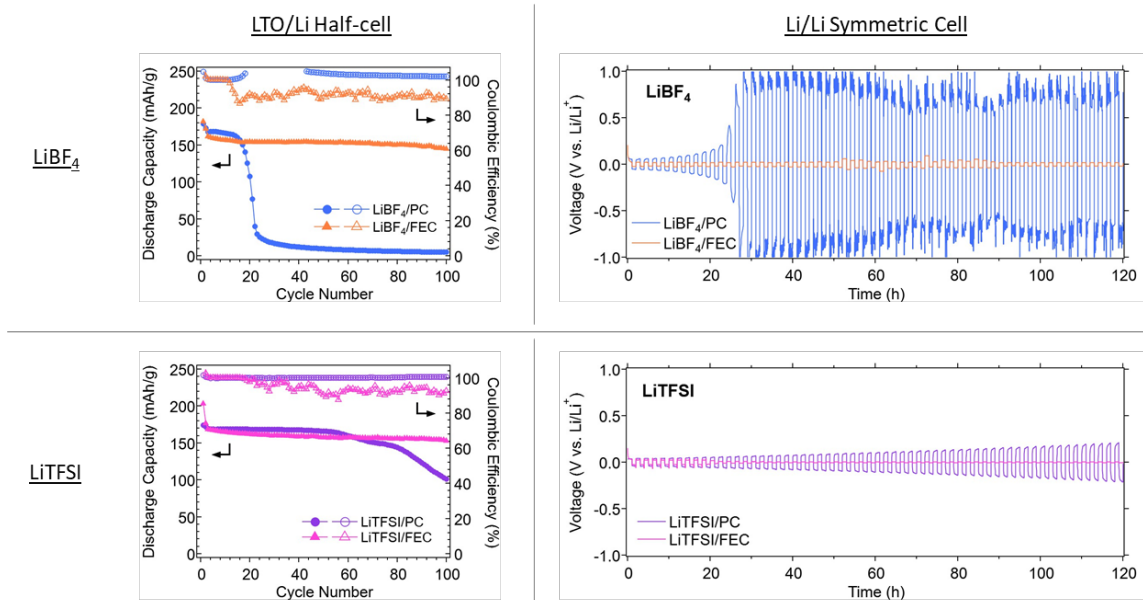
Figure 14. Cycle performance of LTO/Li half cells and Li/Li symmetric cells with LiBF$_4$ in PC and FEC, and LiTFSI in PC and FEC electrolytes. The half cells were cycled at C/10 for 2 formation cycles and at 1C for 100 aging cycles between 1.0 and 2.5 V. The symmetric cells were cycled by applying 2 mA/cm^2 during 1 h half-cycle. All cells were tested at 45°C.

Full-cell test. As the half-cells could not be utilized to test the electrolyte performance, electrolytes were tested with LTO/LMO and LTO/LMNO full cells. LiPF$_6$ and LiBF$_4$ salts with PC and FEC solvent combinations were tested as these electrolytes showed reasonable results in both Al corrosion tests and half-cell tests. The full cells were cycled at C/10 for 2 formation cycles and at 1C for aging cycles. 1.5-3.0 V and 1.5-3.5 V cutoff voltages were used for LTO/LMO and LTO/LMNO cells, respectively. All cells were tested at 45°C. The cycle results are shown in Figure 4. In full cells, PC-based electrolytes performed better than the FEC-based electrolytes with both cathodes, which is opposite from the half-cell results. This result once again confirms that the half-cell result is mainly governed by the Li metal performance. Since FEC can form a favorable, LiF-rich, solid-electrolyte interface (SEI) on the Li metal surface,[7] it results in a better performance than PC that does not have fluorine. Currently, up to ~200 cycles, LiBF$_4$ in PC electrolyte is showing the best performance in the full cells.
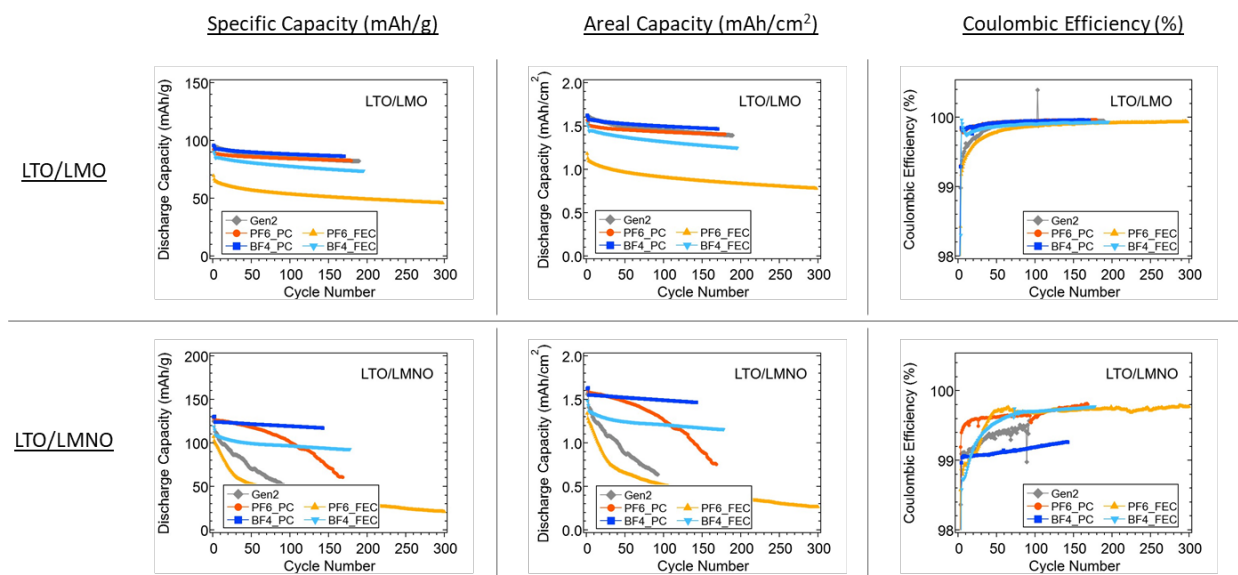
Figure 15. Cycle performance of LTO/LMO and LTO/LMNO full-cells with LiPF$_6$ and LiBF$_4$ in PC and FEC electrolytes. Gen2 electrolyte is shown as comparison. Cells were cycled at C/10 for 2 formation cycles and at 1C for aging cycles. LTO/LMO cells were cycled between 1.5 and 3.0 V and LTO/LMNO cells were cycled between 1.5 and 3.5 V.

Conclusions

Li salt and solvent candidates with different chemical properties were chosen to be screened for LTO anode and Mn-based cathodes. The anodic stability, half-cell performance, and full-cell performance of the selected electrolytes were characterized. From the anodic stability (Al corrosion) tests, LiPF$_6$ and LiBF$_4$ showed wide electrochemical stability window due to the effective passivation of the Al surface, while imide-based salts exhibited narrow stability windows. Half-cell results were strongly affected by the Li metal performance, which was confirmed by Li/Li symmetric-cell tests. Full-cell results showed the opposite trend from the half-cell results, and the current full-cell results show the best performance with LiBF$_4$ in PC electrolyte. In the next quarter, the full cells will continue to be monitored. Moreover, LiFSI and LiOTFAc in PC and FEC combinations will be tested. Although these salts did not show great corrosion test results, the electrolytes will be tested with LTO/LMO cells to check their potentials. Moreover, fluorinated solvents (2,2,2-trifluoroethyl methyl carbonate, bis (2,2,2-trifluoroethyl) carbonate, and 3,3,3-trifluoropropylene carbonate) from ANL will be tested. Finally, Ethylene carbonate (EC) and PC solvent combinations will be tested as it has been reported that the conductivity increases for both LiPF$_6$ and LiBF$_4$ salts as EC is mixed with PC.[8]

References

1. Zhao, B.; Ran, R.; Liu, M.; Shao, Z., A comprehensive review of Li4Ti5O12-based electrodes for lithium-ion batteries: The latest advancements and future perspectives. *Materials Science and Engineering: R: Reports* **2015,** *98*, 1-71.

2. Xu, G.; Han, P.; Dong, S.; Liu, H.; Cui, G.; Chen, L., Li4Ti5O12-based energy conversion and storage systems: Status and prospects. *Coord. Chem. Rev.* **2017,** *343*, 139-184.

3. Zhang, S. S.; Jow, T. R., Aluminum corrosion in electrolyte of Li-ion battery. *J. Power Sources* **2002,** *109*, 458-464.

4. Aravindan, V.; Gnanaraj, J.; Madhavi, S.; Liu, H.-K., Lithium-Ion Conducting Electrolyte Salts for Lithium Batteries. *Chem. - Eur. J.* **2011,** *17*, 14326-14346.

5. Xu, K., Nonaqueous Liquid Electrolytes for Lithium-Based Rechargeable Batteries. *Chem. Rev.* **2004,** *104*, 4303-4417.

6. Tan, S.; Ji, Y. J.; Zhang, Z. R.; Yang, Y., Recent Progress in Research on High-Voltage Electrolytes for Lithium-Ion Batteries. *ChemPhysChem* **2014,** *15*, 1956-1969.

7. Zhang, X.-Q.; Cheng, X.-B.; Chen, X.; Yan, C.; Zhang, Q., Fluoroethylene Carbonate Additives to Render Uniform Li Deposits in Lithium Metal Batteries. *Adv. Funct. Mater.* **2017,** *27*, 1605989.

8. Ding, M. S.; Jow, T. R., How Conductivities and Viscosities of PC-DEC and PC-EC Solutions of LiBF4, LiPF6, LiBOB, Et4NBF4, and Et4NPF6 Differ and Why. *J. Electrochem. Soc.* **2004,** *151*, A2007-A2015.